J Math Chem (2009) 46:532–549
DOI 10.1007/s10910-008-9477-1

ORIGINAL PAPER

Electronic states in ordered and disordered quantum networks: with applications to graphene and to boron nanotubes

N. H. March · G. G. N. Angilella

Received: 19 September 2008 / Accepted: 6 October 2008 / Published online: 25 October 2008

Abstract The idea behind the original quantum network (QN) model is simple enough. One joins each atom to its nearest neighbours, and then treats electrons (though quantum mechanically of course) as though they flowed through one-dimensional wires as in an electrical circuit obeying Kirchhoff's Laws at every node. Here we will begin with two periodic systems: namely a single graphene layer, which has recently been produced experimentally, and a two-dimensional sheet of boron atoms. This will be followed by a discussion of B nanotubes, using the simplest QN model, supplemented by comparison of these results with very recent work of other authors using density functional theory. Then the disordered quantum network (DQN) model will be treated in some detail. First of all, the main, physically motivated, steps by which Dancz, Edwards and March passed from the DQN model to the Boltzmann equation will be set out. They will then be related to substantial progress made on the mathematical solution of the DQN model by a number of authors; again a substantial part of this work invoking the Boltzmann equation.

Invited paper presented at the Workshop "Graph Models of Mesoscopic Systems, Wave Guides, and Nano-Structures (AGAW03)", Newton Institute, Cambridge, UK, April 10–13, 2007.

N. H. March
Oxford University, Oxford, UK

N. H. March
Department of Physics, University of Antwerp, Groenenborgerlaan, 171, 2020 Antwerp, Belgium

G. G. N. Angilella (✉)
Dipartimento di Fisica e Astronomia, Università di Catania, Via S. Sofia, 64, 95123 Catania, Italy
e-mail: giuseppe.angilella@ct.infn.it

G. G. N. Angilella
CNISM, UdR Catania, Catania, Italy

G. G. N. Angilella
INFN, Sez. Catania, Catania, Italy

Keywords Graphene · Quantum networks · Boron nanotubes

1 Background and outline

This study is concerned with electronic states generated by the so-called quantum network (QN) model. This model was devised to investigate conjugated molecules, as summarized in the article by Platt [1], and goes back at least to Pauling [2]. An early contribution to its extension to crystalline solids was that of Coulson [3].

The free electron model of a crystal is that in which the electron travels as a free particle along wires of a network, which in turn is fitted on to the crystal lattice. The wires represent 'bonds' (e.g. in a graphene layer to be discussed a little further below) and the nodes of the network represent atoms. More realistically, potentials can be put along the lines of the network, examples being given in Refs. [4–7]. This addition of potentials is done in such a way that each node of the network lies in the centre of a well. To provide a concrete background to what follows, we shall below give a summary of Montroll's model as it can be fully solved analytically. In the course of this article, we shall present our own contributions to the chemists network model. Then we shall make numerous comments involving very recent studies by a variety of authors.

It is natural to begin with the spatially ordered network model, and the prime focus will be on results for boron. However, it will prove useful to introduce the boron results by referring, albeit briefly, to our own π-electron calculations relating to a graphene layer, the interest in this material having been hugely re-kindled since its synthesis [8–10] (see also Ref. [11] for a recent review).

The outline of the present article is then as follows. In Sect. 2, the electronic structure of boron, both in layer and in nanotube geometries, will be discussed. After this discussion of boron, based as it was on the Laplace operator, the gross effects of bond potentials will be treated, following Klein and March [7], appeal also being made to the studies of other authors (see especially the very recent bond potential work of Kuchment and Post [12]; for carbon, some contact is made between their study and results from the simple Laplace operator treatment.

Then the final part of this article will be concerned with disordered networks, a field which has grown rapidly fairly recently. As background to such developments over the past decade, the steps involved in the early physically motivated proposal by Dancz et al. [13] to treat such disordered networks by appealing to the Boltzmann transport equation will first be set out. Following this, we shall refer, albeit more briefly, to important recent progress on the random network model made by authors including in particular Germinet [14], Aizenman [15–17], Veselić [18], and Exner [19]. We shall also refer to results obtained by Schrader et al. [20] on the interesting model these workers termed a 'random necklace'.

1.1 Electron states in Montroll's model

Montroll [5] considered a quantum particle moving in a network, with aperiodic and periodic networks representing molecules and crystals, respectively. While he

neglected the dynamics of the network nodes, fixed at the nuclei positions, he restricted the problem to that of finding the wave function of the particles only along the bonds connecting nodes in the network. Such an approximation reduces a generally multidimensional problem to an inherently one-dimensional problem. For particular choices of the potential acting on the particle along the bonds, the problem turns out to be exactly solvable, thus allowing one to extract relevant information, such as energy bands and density of states. Montroll [5] originally assumed that the potential wells along the bonds give rise to a single electronic bound state for each node. He later extended his model to the case of several bound states per node [6].

What is essential to Montroll's model is that the particle wave functions along each bond should match continuously at a node. In addition, momentum or current conservation implies that $\sum \nabla\phi = 0$, where the gradient of the wave function ϕ is measured along each network bond away from a given node. Such a condition ('Kirchhoff law') amounts to a set of homogeneous equations

$$F(k,\eta)\phi[j] = \sum_{i=1}^{c} \phi[j_i], \tag{1}$$

where $\phi[j]$ is the wave function along the network bond j, the summation on the right hand side is restricted to all bonds j_i connecting a given node to its c nearest neighbours, and $F(k,\eta)$ is a matrix form factor, depending on particle's momentum k and the parameters η characterizing the atomic potential acting on the particle. It is immediate to recognize a formal analogy with the usual textbook model of masses and springs, to describe the vibrations of a lattice.

Montroll [6] then proceeds to discuss the case of a potential well $V(x) = -V_0 \operatorname{sech}^2 \gamma x$, interpolating between the limit of nearly localized ($\gamma \to \infty$) and free ($\gamma = 0$) particles. The quantum problem corresponding to such a potential $V(x)$ can be solved analytically. In particular, the density of states (DOS) in any dimensions can be connected with the form factor, and shows analytical similarities with the DOS calculated within, say, the tight binding model. Specifically, the DOS is characterized by Van Hove singularities in dimensions $d \leq 2$, corresponding to the Fermi manifold touching the boundaries of the Brillouin zone, and to a change of its topology.

2 Results for a single graphene layer and for a two-dimensional sheet of boron atoms

In this section, we treat two periodic two-dimensional assemblies, namely (i) a single graphene layer (which can now be produced experimentally [8–10]; see also Ref. [11] for a recent review), and (ii) a sheet of boron atoms.

2.1 Quantum currents in networks

Quantum mechanics on a generally multiply connected lattice can be reformulated in terms of the corresponding covering space, which contains all non-homotopic paths

in the original lattice, i.e. paths that cannot be deformed into one another [21]. The covering space is locally like the original lattice but is simply connected. The covering space of a lattice network is essentially obtained by eliminating all closed loops.[1] In the case of a (discrete) network or lattice, the covering space is given by an infinite or Cayley tree, which is essentially one-dimensional. Ringwood's approach [21] enables the Green's function of a free particle on a lattice to be expressed as a sum over all distinct homotopic paths.

Let us assume that at time $t = 0$ the particle can be located at a particular point of the line segments of the tree. For $t > 0$ it will then evolve freely along the one-dimensional path connecting the original point to one of its c neighbouring nodes in the tree. At a node, the wave function is required to vary continuously, whereas the current divides equally down the remaining $c - 1$ branches. The wave function $\psi(x)$ and $(c-1)^{-1}\partial\psi/\partial x$ evaluated at the node act therefore as initial conditions for the wave function in the next $c - 1$ segments. These are the so-called Griffith's boundary conditions [21], and correspond to the Kirchhoff's laws of classical circuits [22].

Let $\omega = \sqrt{-E}$, with $E < 0$ the particle's energy. Then, the Green's function between two points at a distance y apart along the same line segment reads $G(y) = -(2\omega)^{-1}e^{-\omega|y|}$. The Green's function between two points P and P' at a distance x and x' from the original node and separated by N nodes in the tree (T), can then be obtained as

$$G_T(x, x'; E) = (e^{-\omega x'}\ e^{\omega x'})Z(b_{N-1})Z(b_{N-2})\ldots Z(b_1)Z(x)\begin{pmatrix}\frac{1}{2\omega}\\ 0\end{pmatrix}, \qquad (2)$$

where b_i is the length of the ith segment in the tree and

$$Z(b) = \frac{1}{2(c-1)}\begin{pmatrix} ce^{-\omega b} & (c-2)e^{\omega b}\\ (c-2)e^{-\omega b} & ce^{\omega b}\end{pmatrix}. \qquad (3)$$

The Green's function on the lattice (L) is then obtained by a sum over all homotopically distinct walks γ connecting P and P' as

$$G_L(x, x'; E) = \sum_{\gamma} e^{i\alpha(\gamma)}G_T(\gamma x, x'; E), \qquad (4)$$

where $\alpha(\gamma)$ enters the phase of the wave function through $\psi(\gamma x) = e^{i\alpha(\gamma)}\psi(x)$.

Ringwood [21] uses the results outlined above to recover the (more directly calculated) density of states in a graphene layer given by Coulson [3,4]. In a little more detail, Ringwood [21] writes the dispersion relation $E = E(\mathbf{k})$ implicitly as

$$c\cos(E^{1/2}a) = S(\mathbf{k}), \qquad (5)$$

[1] Ringwood [21] exemplifies the real line (a simply connected one-dimensional space) as the universal covering space of the circle: they are locally indistinguishable, but the real line can be thought of as infinite copies of the circle, obtained by rolling the circle without slipping along the real line.

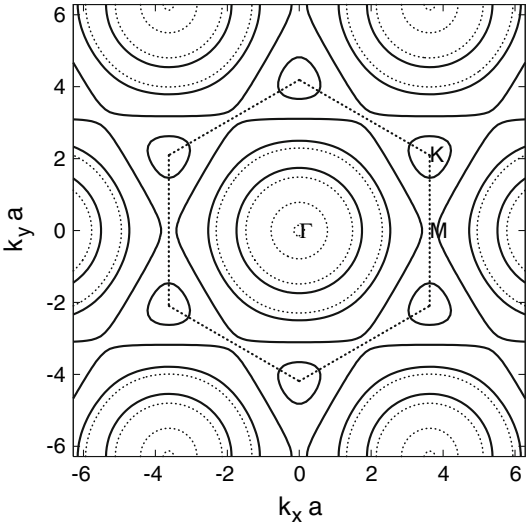

Fig. 1 Dispersion relation within Ringwood's approach [21] for a graphene layer. it Solid and *dashed lines* refer to valence and conduction bands for π-electrons in the graphene sheet, respectively. *Dashed hexagon* marks the boundaries of the 1BZ, with special points $\Gamma \equiv (0, 0)$, $M \equiv (2\pi/a\sqrt{3}, 0)$, $K \equiv (2\pi/a\sqrt{3}, 2\pi/3a)$

where c is the coordination number ($c = 3$ for graphene) and $S(\mathbf{k}) = \sum_{j=1}^{c} e^{i\mathbf{k}\cdot\mathbf{a}_j}$ is the local structure factor, $\mathbf{a}_j$ being the lattice vectors connecting a node to its c neighbours, at a distance a (cf. Eqs. 9 and 10 below). The dispersion relation for a graphene layer is plotted in Fig. 1 as contour lines of $E(\mathbf{k})$ as given by Eq. 5. Ringwood [21] then expresses the density of states corresponding to such a dispersion relation as

$$N(E) = -\frac{1}{\pi}\,\mathrm{Im}\,\frac{\sinh\omega a}{\omega}\,\frac{1}{(2\pi)^d}\int\frac{d^d\mathbf{k}}{c\cosh\omega a - E(\mathbf{k})}, \tag{6}$$

where $\omega = (-E^+)^{1/2}$, and $d = 2$ for a graphene layer. We have in Fig. 2 plotted our results for $N(E)$, calculated by means of Ringwood's approach for a graphene layer.

2.2 Electronic states in a two-dimensional sheet of boron (B) atoms

Leys et al. [23] considered states having different chiralities, and explicitly derived the one-dimensional (1D) energy bands of a number of foldings of the 2D boron sheet discussed above. Below, we consider the case of a (n, n) i-zigzag boron nanotube.

2.2.1 One dimension

Within the orientation selected for the x–y coordinate system, the chiral vector $\mathbf{C}_h$ (and correspondingly the reciprocal lattice vector $\mathbf{K}_1$) is directed along the positive x axis for this special case of (n, m) chosen such that $m = n$. Using periodic boundary conditions along the circumferential direction then yields

$$k_{x,j} = \frac{2\pi}{n\sqrt{3}a}, \quad j = 1, \ldots, 2n. \tag{7}$$

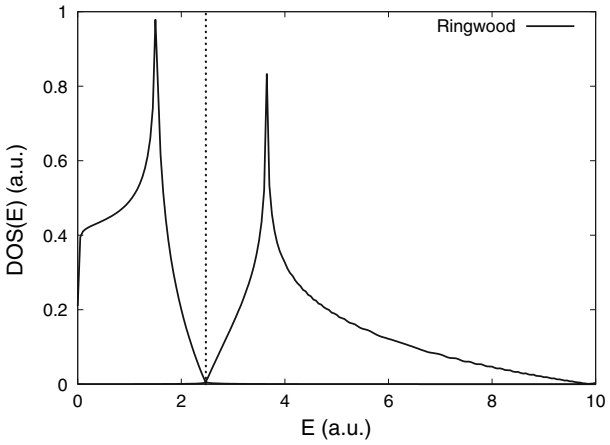

Fig. 2 Density of states within Ringwood's approach [21] for a graphene layer. The *vertical line* marks the location of the Fermi level, lying precisely between the valence and conduction bands for π-electrons in the graphene sheet. This DOS reproduces the one originally derived by Coulson [3], using a quite different method, for a graphene layer within the QN model

Then the i-zigzag structure factor $S_j^{iz}(k)$ which results is given by

$$S_j^{iz}(k) = 2\cos ka + 4\cos\left(\frac{\pi j}{n}\right)\cos\left(\frac{ka}{2}\right), \tag{8}$$

where $j = 1, \ldots, 2n$ and $-\pi/a < k < \pi/a$. From this result, one can readily write the corresponding equation for the (n, n) energy bands $E_q^{iz}(k)$ for the QN model.

Figure 3 (left) displays the energy bands obtained for a boron (3, 3) i-zigzag nanotube which has a diameter of 5.20 a. The fact that $\mathbf{K}_1$ is directed along a symmetry axis of the 2D Brillouin zone has the consequence that the energy bands are symmetrical around the origin. The tight-binding model has been found to have a similar set of energy bands, as well as the same general form and degeneracy.

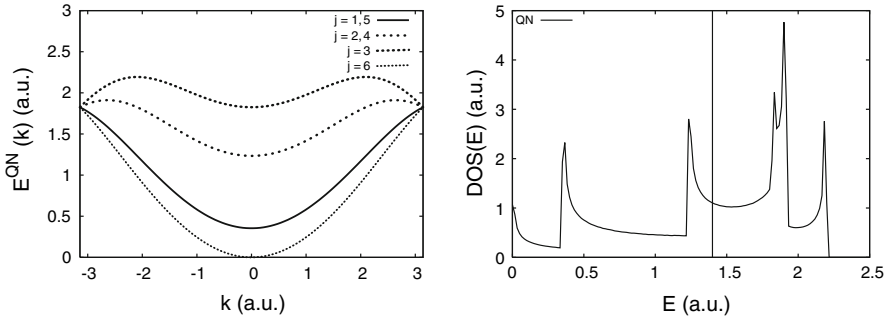

Fig. 3 *(Left)* Energy bands for a boron (3, 3) i-zigzag nanotube, within the QN model. *(Right)* Density of states for a (3, 3) i-zigzag boron nanotube, within the QN model, corresponding to the energy bands displayed in this figure. The vertical line denotes the Fermi level (half occupied band) (cf. Ref. [23])

Corresponding to the energy bands in the left panel of Fig. 3, the right panel of the same Fig. 3 displays the cumulative DOS for such a 1-D boron (3, 3) *i*-zigzag nanotube. The various Van Hove singularities are to be associated with the crossover from one band to another, and correspond to $j = 6$, $j = 1, 5$, $j = 2, 4$, $j = 3$, $j = 2, 4$, and $j = 3$, from left to right.

2.2.2 Two dimensions

Leys et al. [23] have given a detailed derivation of the dispersion relation $E(\mathbf{k})$ for such a B sheet, via the QN model. This reads:

$$E(\mathbf{k}) = \frac{q^2}{2} = \frac{1}{2}\left[\frac{1}{a}\arccos\left(\frac{1}{c}S(\mathbf{k})\right)\right]^2. \tag{9}$$

The local structure factor appearing in Eq. (9) is defined by

$$S(\mathbf{k}) = \sum_{j=1}^{c} e^{i\mathbf{k}\cdot\mathbf{a}_j}, \tag{10}$$

where the vectors $\mathbf{a}_j$ are such that they connect every lattice point $\mathbf{R}$ to its c nearest neighbours. For comparison with Eq. 9 on the QN model, the tight-binding dispersion relation turns out to have the form

$$E^{\mathrm{TB}}(\mathbf{k}) = \epsilon_\pi + tS(\mathbf{k}). \tag{11}$$

If ϕ_π denotes the atomic π-orbital centred on lattice position $\mathbf{R}_i$, then ϵ_π is the matrix element $\langle\phi_\pi(\mathbf{r})|H|\phi_\pi(\mathbf{r})\rangle$, where H is the Hamiltonian, while t in Eq. 11 is given by

$$t_i \equiv t = \langle\phi_\pi(\mathbf{r} - \mathbf{a}_i)|H|\phi_\pi(\mathbf{r})\rangle, \quad i = 1, \ldots, 3. \tag{12}$$

The two methods share analytical similarities.

Returning to the QN model leading to $E(\mathbf{k})$ in Eq. 9, the density of states can be obtained as

$$\mathrm{DOS}(E) = \frac{2}{(2\pi)^2}\int \frac{ds}{|\nabla_{\mathbf{k}}E(\mathbf{k})|}, \tag{13}$$

where the line integral is along a contour of constant energy E. We record the results for both the TB and the QN models in Fig. 4, where the band parameters ϵ_π and t in the TB case have been chosen in such a way as to have the band extrema coincide with the QN case. While the DOS of the two models share common analytical features, such as the occurrence of a Van Hove singularity, with a logarithmically divergent DOS, corresponding to a change of topology of the Fermi line, it can be seen that the TB model slightly overestimates the location of both the Fermi level and the Van Hove singularity, with respect to the QN case.

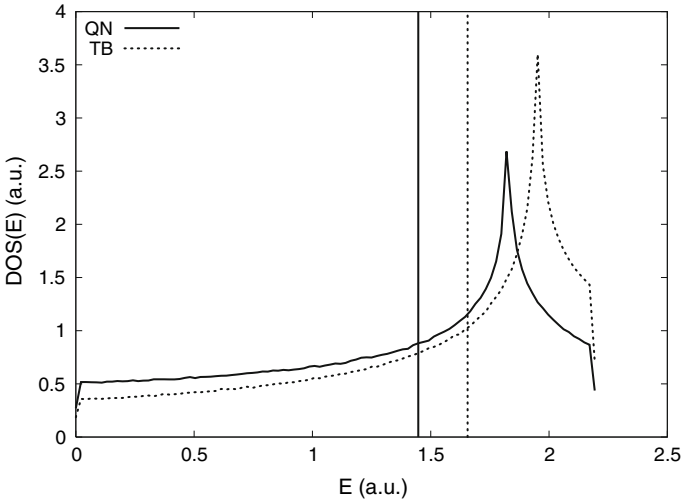

Fig. 4 Density of states for the boron sheet, within the quantum network (QN, *solid line*) and the tight binding (TB, *dashed line*) models. *Vertical lines* mark the position of the Fermi level in either case (half occupied band)

3 Electronic structure of B nanotubes from the quantum network model

One needs, of course, to specify the model B 2D lattice, which is assumed planar, and which will eventually be folded to obtain B nanotubes. The structure of the B sheet considered can be simply obtained by considering an ordinary sheet of graphene in which (a) all C atoms are replaced by B atoms, and (b) an additional B atom is placed in the centre of each hexagon. The result is then that every B atom has a near-neighbour coordination, denoted by c, which is equal to 6. Fig. 5 shows the resulting lattice.

This lattice is described by using two lattice vectors, $\mathbf{a}_1$ and $\mathbf{a}_2$, which are either 120° apart of 60° apart. If one wishes only to describe the 2D lattice, both choices prove equivalent. However, we wish below to employ these lattice vectors to characterize the nanotubes obtained by folding the 2D sheet. Then it turns out that the choice where both lattice vectors are 60° apart is the most useful.

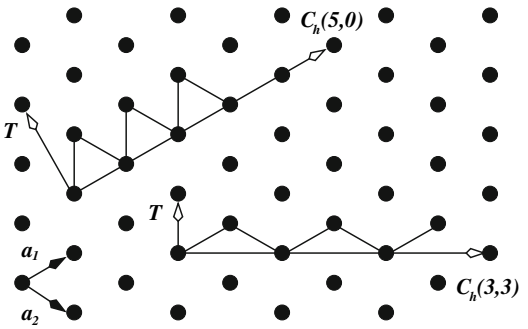

Fig. 5 Lattice structure of a B sheet, with chiral vectors $\mathbf{C}_h(n, m)$ for the realization of two possible nanotubes, upon folding

To describe a nanotube constructed by folding such a sheet of B atoms, the starting point is to define a chiral vector $\mathbf{C}_h$ such that

$$\mathbf{C}_h = n\mathbf{a}_1 + m\mathbf{a}_2. \tag{14}$$

This vector connects, by definition, two lattice points on the sheet which have to be connected on folding to form a tube. The specific choice of the pair (n, m) then completely determines the structure of the tube which is thereby produced. From the definition of the chiral vectors $\mathbf{C}_h$, it follows that its length, which equals the circumference, L say, of the resulting nanotube, is given by

$$L = a\sqrt{n^2 + m^2 + nm}. \tag{15}$$

All possible distinct seamless nanotubes can be constructed by choosing (n, m) with n any integer and m ranging from 0 to n. We simply note here that, dealing with boron, both the nanotube generated by a $\mathbf{C}_h(n, n)$ chiral vector and that generated by a $\mathbf{C}_h(n, 0)$ vector have in essence zigzag symmetry. In the case $n = m$, one has however isosceles triangles (i), while in the case $m = 0$ we have equilateral triangles (e). We refer below to these limiting choices as (n, n) i-zigzag and $(n, 0)$ e-zigzag symmetry, respectively.

3.1 Definition of unit cell of B nanotube

We need next to define both the unit cell and the corresponding Brillouin zone of the B nanotube. It parallels the C case, which is set out in Ref. [24].

The vector perpendicular to the chiral vector $\mathbf{C}_h$ going from the (chosen) origin to the nearest lattice point defines the translational vector of the 1D periodic nanotube. This is

$$\mathbf{T} = t_1\mathbf{a}_1 + t_2\mathbf{a}_2, \tag{16}$$

the relation between t_1, t_2 and m, n being unchanged from the C case, for which

$$t_1 = \frac{2m + n}{d_R}, \quad t_2 = -\frac{2n + m}{d_R}, \tag{17}$$

d_R being the greatest common divisor (gcd) of $2m + n$ and $2n + m$. The rectangle generated by $\mathbf{C}_h$ and $\mathbf{T}$ constitutes the unit cell of the B nanotube, where the translational vector $\mathbf{T}$ determines the direction in which the unit cell repeats itself periodically.

3.2 Reciprocal space and Brillouin zone

The reciprocal lattice vector $\mathbf{k}_1$ and $\mathbf{k}_2$ are defined by

$$\mathbf{b}_i \cdot \mathbf{a}_j = 2\pi\delta_{ij}. \tag{18}$$

The vectors in the reciprocal space of the nanotube are defined by the relations

$$\mathbf{C}_h \cdot \mathbf{K}_1 = 2\pi \ : \ \mathbf{T} \cdot \mathbf{K}_1 = 0, \tag{19a}$$

$$\mathbf{C}_h \cdot \mathbf{K}_2 = 2\pi \ : \ \mathbf{T} \cdot \mathbf{K}_2 = 2\pi. \tag{19b}$$

This results for $\mathbf{K}_1$ and $\mathbf{K}_2$ in the forms

$$\mathbf{K}_1 = \frac{1}{N}(-t_2\mathbf{b}_1 + t_1\mathbf{b}_2), \tag{20a}$$

$$\mathbf{K}_2 = \frac{1}{N}(m\mathbf{b}_1 - n\mathbf{b}_2), \tag{20b}$$

where N is given by

$$N = mt_1 - nt_2 = \frac{|\mathbf{C}_h \times \mathbf{T}|}{|\mathbf{a}_1 \times \mathbf{a}_2|} = \frac{2(m^2 + n^2 + mn)}{d_R}. \tag{21}$$

Here, $\mathbf{b}_1$ and $\mathbf{b}_2$ are the lattice vectors of the graphene Brillouin zone (BZ), while N is the number of atoms in the unit cell of the nanotube. It should be noted that for the C case the number of C atoms in the nanotube unit cell is $2N$.

Since the B nanotube is periodic only in one dimension, only the vector $\mathbf{K}_2$ is a reciprocal vactor defining a 1D BZ. Along the direction of $\mathbf{K}_1$, periodic boundary conditions will result in a quantization of the component of the wave vector in that direction. Each allowed value will then contribute a 1D energy band in the 1D BZ.

It is to be noted that since the B lattice we consider here can be constructed from taking only the lattice points in a graphene layer (points with identical environment), the BZ of the B and C sheets have identical symmetries.

It is relevant to note that Leys et al. [23,25] have used the QN model to treat C cages and nanotubes. However, below, we refer briefly to the subsequent studies of Kuchment and Post (KP) [12] and Badanin et al. [26,27]. Both studies consider the Schrödinger operator with a periodic potential, KP giving an explicit derivation of dispersion relations on C nanostructures, including graphene treated above and all types of single-wall nanotubes. The later studies of Badanin [26,27] focus on armchair single-wall nanotubes.

While there is an intimate connection between the KP study [12] and the later work of Badanin et al. [26,27], as is pointed out in the latter, the case treated by KP of even potential is such that the spectrum of the Schrödinger operator on the nanotubes considered coincides with the spectrum of the Hill operator, as proved by KP. Badanin et al. relate this finding to the corresponding Lyapunov function for even potential being expressible in terms of that function for the Hill operator. Beyond the achievements of KP summarized very briefly above, Badanin et al. provide spectral analysis for the Schrödinger operators with arbitrary potentials on edges.

We refer next, albeit briefly, to recent work of Cabria et al. [28]. These authors have treated B sheets by a version of density functional theory (DFT), the geometric as well as the electronic structure now being explored. The DFT results were obtained with a computational procedure using plane-waves and ultrasoft pseudopotentials.

For the exchange-correlation potential, Cabria et al. used the local density approximation (LDA) functional of Vosko et al. [29] and the generalized gradient approximation (GGA) functional of Perdew et al. [30]. The stable geometry of a B sheet is then found to exhibit buckling. Two different B–B bond lengths characterize the geometry with buckling: (i) 1.63 Å between the B atoms in a row, and (ii) 1.81 Å between the B atoms in adjacent rows. Although buckled and planar B sheets have rather different bonding characteristics, an essential similarity of the electronic structure is that both are metallic.

Cabria et al. [28] demonstrate further that B nanotubes (BNTs) produced by rolling up a B sheet have also a buckled surface when the helicity permits the formation of alternating up and down B rows in the surface. However, in all other examples, BNTs exhibit only flat surfaces, as assumed in our own work. Again, buckled B and the corresponding nanostructures have the common feature that their electronic states both correspond to metallic phases.

4 Electronic structure of a disordered quantum network

In the work of Dancz et al. [13], a solid composed of a single quadrivalent atomic type is again considered as for, say, graphite, but the use of Bloch's theorem for periodic arrays was replaced by statistical considerations to take account of the topological and positional disorder. At the heart of the statistical approach was to consider the network as an array of intersecting paths. These paths can then be compared to the trajectories of particles in a perfect gas, the intersection representing the analogue of collisions. This then suggested that one should invoke a Boltzmann equation, whose validity would be analogous to the series of approximations associated with the customary Boltzmann equation. Following this discussion, we shall consider briefly the work of Ziman [31] and the subsequent study of Dancz et al. [32,33].

4.1 Sketch of arguments leading to the Boltzmann equation

As in the ordered QN model, electrons move along lines joining near-neighbour atoms. The boundary conditions appropriate to the wave functions associated with a quadrivalent (or other valency) atom have been discussed, e.g., by Ruedenberg and Scherr [34] (see also Refs. [35–37]). These boundary conditions take the form that (i) the wave function ψ is continuous across an intersection and therefore ψ on each of the four paths satisfies

$$\psi_1 = \psi_2 = \psi_3 = \psi_4; \tag{22}$$

and (ii) the sum of the derivatives, as measured away from the intersection, must vanish, and hence one has

$$\psi_1' + \psi_2' + \psi_3' + \psi_4' = 0. \tag{23}$$

It is useful to work with the logarithmic derivative $z(x, E)$ along a path x, as measured from one intersection to the next, and defined explicitly by

$$z(x, E) = \frac{1}{\psi(x, E)} \frac{\partial \psi(x, E)}{\partial x}. \tag{24}$$

Equations 22 and 23 may then be rewritten as

$$z_1(x, E) + z_2(x, E) + z_3(x, E) + z_4(x, E) = 0. \tag{25}$$

Of course, in the basic QN model, on each of these paths the wave function obeys the free electron Schrödinger equation (in atomic units with $\hbar = m = 1$)

$$\left[\frac{1}{2}\frac{\partial^2}{\partial x^2} + E\right]\psi(x, E) = 0. \tag{26}$$

The equation of motion for the logarithmic derivative $z(x, E)$ readily follows from Eqs. 24 and 26 as

$$\frac{\partial z(x, E)}{\partial x} + z^2(x, E) + 2E = 0. \tag{27}$$

The next important step (see Ref. [13]) is to define a joint probability distribution, which is denoted by $P(x_0, \psi_0, x)$ for the probability that

$$\psi(x, E) = \psi_0 \quad \text{and} \quad z(x, E) = z_0 \tag{28}$$

at a point x along the path. Following the assumptions of Dancz et al. [13], the properties of this probability distribution can be determined from the Liouville equation

$$\left[\frac{\partial}{\partial x} + \frac{\partial}{\partial \psi}(z\psi) - \frac{\partial}{\partial z}(z^2 + 2E)\right] P(z, \psi, x) = 0 \tag{29}$$

together with the boundary conditions at an intersection.

4.2 Passage from the Liouville equation to the Boltzmann equation for the disordered QN model

If the network is next considered to be made up of paths, one may follow Dancz et al. [13] in writing down a Boltzmann equation for this model, by assigning a direction to the paths and thereby defining a sense to the x's. This turns out to be always possible for a $2N$-valent species. Then, as one traverses one of these paths, there is a pair (z, ψ) just before an intersection and a pair (z', ψ') just after. The changes in these functions, of course, are due to the influence of the intersecting path with another (z_1, ψ_1) just before and a (z_1', ψ_1') just following the intersection. Following Dancz et al. [13] let us

emphasize this analogy by changing to customary Boltzmann equation notation via the correspondence

$$[z, \psi;\ z', \psi';\ z_1, \psi_1;\ z_1', \psi_1'] \to [v, r;\ v', r';\ v_1, r_1;\ v_1', r_1']. \tag{30}$$

Then Eq. 22 is analogous to the assertion that the particles of a perfect gas are points with a zero range of interaction. Dancz et al. [13] further assume that (i) there is no correlation between the values of v, v_1, v_1', and (ii) there is a distribution of path lengths between intersections so that the knowledge of a previous 'collision' can be considered, on average, lost. Then, it may be anticipated that a Boltzmann transport approach will be applicable. The 'scattering' term, however, may be expected to differ from the usual equation, since the values of v, v_1 classically determine v', v_1' given the impact parameter: for the present disordered QN model these conditions are not sufficient and an additional boundary condition which defines v_1' is required. Dancz et al. [13] therefore argue that the probability of finding v_1, r_1 is determined by the network lying behind the intersection along the v_1, r_1 path. A similar argument for v_1', r' also holds and then one is directly led to a Boltzmann equation which reads [13]

$$\left[\frac{\partial}{\partial x} + \frac{\partial}{\partial \psi}(z\psi) - \frac{\partial}{\partial z}(z^2 + 2E)\right] P(z, \psi, x) = \rho \mathcal{L}[P(z, \psi, x)], \tag{31}$$

where ρ is the average density of intersections per unit length, while $\mathcal{L}[f(z, \psi)]$ is a linear functional given by

$$\begin{aligned}\mathcal{L}[f(z, \psi)] = \Bigg[&\int\int dz_1 d\psi_1\, P(z_1, \psi_1) \int\int dz_1' d\psi_1'\, P(z_1', \psi_1') \\ &\times \int\int dz' d\psi'\, \delta(z - z' + z_1 - z_1')\delta(\psi - \psi_1)\delta(\psi - \psi')\delta(\psi - \psi_1') \\ &\times \big(f(z', \psi') - f(z, \psi)\big)\Bigg] \Bigg/ \left[\int dz'\, P(z', \psi)\right]^2 .\end{aligned} \tag{32}$$

It is to be noted that the wave function does not enter the 'scattering' term just as the scattering process is position independent in the Boltzmann gas. Furthermore, as in the Boltzmann gas, the joint probability distribution $P(z, \psi, x)$ rapidly approaches a steady state independent of x. Thus Eq. 31 takes the simpler form

$$\left[\frac{\partial}{\partial \psi}(z\psi) - \frac{\partial}{\partial z}(z^2 + 2E)\right] P(z, \psi) = \rho \mathcal{L}[P(z, \psi)] \tag{33}$$

and therefore the quantity $P(z, \psi)$ can be determined self-consistently. Integrating over ψ in Eq. 33, one finds the probability $P_0(z)$ of finding the value of z in the steady state to be governed by the equation

$$-\frac{\partial}{\partial z}(z^2+2E)P_0(z)=\rho\int dz_1\,P_0(z_1)\int dz_1'\,P_0(z_1')\times\int dz'\,\delta(z-z'+z_1-z_1')[P_0(z')-P_0(z)]. \quad (34)$$

Here use has been made of the fact that ψ and z are statistically independent. The Boltzmann counterpart to this condition is that the velocity distribution is not a function of the coordinates.

A Fourier transform of $P_0(z)$, say $\tilde{P}_0(\omega)=\int dz e^{i\omega z}P_0(z)$, leads to a simplification of Eq. 34. Since $P_0(z)$ is a probability distribution, the Fourier transform $\tilde{P}_0(\omega)$ satisfies the condition $\tilde{P}_0(0)=1$ and $\tilde{P}_0(-\omega)=\tilde{P}_0^*(\omega)$. Then Eq. 34 becomes

$$\left[\frac{\partial^2}{\partial\omega^2}-2E+\frac{i\rho}{\omega}\left(|\tilde{P}_0(\omega)|^2-1\right)\right]\tilde{P}_0(\omega)=-2\pi N(E)\delta(\omega). \quad (35)$$

This Eq. 35 is the central result of the Dancz et al. [13] approximate theory of a disordered QN model. The quantity $N(E)$ appearing in Eq. 35 arises from the asymptotic behaviour of $P_0(z)$ and is given precisely by the limiting form

$$\lim_{z\to\pm\infty} z^2P_0(z)=N(E). \quad (36)$$

For a one-dimensional system, Frisch and Lloyd [38] have shown that the quantity $N(E)$ is the cumulative density of states.

As Dancz et al. [13] show, an approximate solution for $\tilde{P}_0(\omega)$ in Eq. 35 can be obtained by self-consistently expanding in a power series about the origin

$$\tilde{P}_0(\omega)=1+[-\pi N(E)+i\alpha]\omega+[E+i\pi\rho N(E)]\omega^2+\cdots, \quad (37)$$

where α is to be chosen such that the series convergese for large ω. If one now introduces the quantities γ and θ through the definitions

$$\gamma=2E+2\pi i\rho N(E) \quad (38a)$$
$$\theta=\rho(2E+\pi^2N^2(E)+\alpha^2), \quad (38b)$$

Equation 35 becomes, to first order in ω,

$$\left(\frac{\partial^2}{\partial\omega^2}-\gamma+i\theta\omega\right)\tilde{P}_0(\omega)=-2\pi iN(E)\delta(\omega). \quad (39)$$

This Eq. 39 has a solution which is a linear combination of Airy functions. Equation 39 can also be transformed back to obtain for $P_0(z)$:

$$\left[\theta\frac{\partial}{\partial z}+(z^2+\gamma)\right]P_0(z)=N(E), \quad (40)$$

with solution

$$P_0(z) = N(E)e^{-\frac{1}{\theta}\left(\frac{1}{3}z^3+\gamma z\right)} \int_{-\infty}^{z} d\mu\, e^{+\frac{1}{\theta}\left(\frac{1}{3}\mu^3+\gamma\mu\right)}. \tag{41}$$

The 'density of states' $N(E)$ can then be obtained from the normalization condition.

As emphasized by Dancz et al. [13], Eqs. 39–41 are equivalent to what Halperin [39] obtained for an electron in a random white-Gaussian noise potential. By following the methods of Halperin, the density of states plus the density matrix can be found. Also, in his formalism, two-point density matrices and electrical conductivity can be discussed.

To conclude this section, it is worthy of emphasis that the power series expansion in ω assumed in Eq. 37 is inessential, the non-linear differential Eq. 35 being amenable to numerical solution.

4.3 Beyond the Dancz et al. model

Prompted by the work of Dancz et al. [13], it has been pointed out by Ziman [31] that care is needed to avoid some indeterminacy in the probability distribution $P(z)$ of the logarithmic derivatives of the wave function.

We note at this point that two basic approximations are involved in the Dancz et al. [13] treatment which leads to a Boltzmann equation for a disordered QN. The first is equivalent to the neglect of closed circuits. Put in mathematical terms, the network is a disordered Cayley tree, i.e. there is one and only one path joining any two points in the network. There seem to be physical systems analogous to this. Thus vulcanized rubber has perhaps some hundreds of monomer units between each vulcanizing link and such a weakly linked system might be expected to be well described by a Cayley tree. Of course, the other extreme of a perfect crystal which has infinitely many regular closed circuits would be very badly represented by a Cayley tree.

Returning at this point to the considerations of Ziman [31], Dancz has argued that additional conditions on ψ at the surface of the tree structure are taken into account in the Dancz et al. [13] analysis. The Ziman proof of complete indeterminacy is valid only for an infinite network, where there are no end conditions to be statisfied on any chain. But further studies are needed in this area as Ziman stresses [31].

It is important here to refer to the subsequent treatment of Dancz and Edwards [32]. In this study, a logarithmic derivative propagator is derived [see their Eq. 2.10]. They then note that this propagator yields the result of Dancz et al. [13], using the Boltzmann transport equation for a tetravalent Cayley tree with randomly occurring (e.g. uncorrelated) intersections.

Also relevant to the above discussion is the later investigation [33] of the electronic structure of disordered networks by utilizing and extending the techniques of Halperin [39]. In this study of Dancz and Edwards [33] one specific result is to obtain an averaged local density of states which reproduces the result of Lloyd [40] for a Cayley tree of fixed connectivity with Lorentzian disorder.

4.4 Transcending the Boltzmann equation approach

While various authors have subsequently confirmed the relevance and utility of the Boltzmann equation approach of Dancz et al. [13] to treat the DQN, much mathematical progress has come subsequently from a more general approach to the problem of localization on quantum graphs produced by a random potential.

Among the most recent contributions on the above mathematical area, we choose to mention within the present context especially those with extensive bibliography. Thus, Exner et al. [19] have used multiscale analysis to prove spectral and dynamical localization for the specific case of a cubic lattice quantum graph with a random potential. Such multiscale analysis in relation to localization in random media is reviewed in earlier work of Germinet and Klein [41] (see also Ref. [42]). Subsequent to these two reviews, Aizenman et al. [15] have used moment analysis (more precisely, analysis of fractional moments of the resolvent) to study localization effects of disorder on the spectral and dynamical properties od Schrödinger operators with random potentials. The results these workers derive include exponentially decaying bounds on the transition amplitude and related projection kernels. Fractional moments are finite due to the resonance-diffusing effects of disorder. Related recent work on the spectrum of random Schrödinger operators on tree graphs is that of Aizenman et al. [16] and of Aizenman and Warzel [17]. Dimensional dependence of localization, referred to by Dancz et al. [13], has been reopened recently by Germinet et al. [14]. For an attractive Poisson random potential in any dimension, these authors prove exponential and dynamical localization at low energies for the Schrödinger operator. They also find that the eigenvalues in that spectral region of localization have finite multiplicity. Following the early discussion by Dancz et al. [13] on the integrated density of states, we note also here the extensive recent review with this quantity at its focus, by Veselić [18].

Kostrykin and Schrader considered the so-called random necklace model [20]. Again, one focus of their work was the integrated density of states, another being the study of the Lyapunov exponent for the random necklace model. These authors studied such a model which they think may provide the simplest example of a differential operator on a nontrivial infinite random metric graph. The graph consists of infinitely many loops joined symmetrically by intervals of unit length, such that the arc lengths of the loops are independent, indentically distributed random variables. Their terminology of a random necklace model was then motivated by the model of Avron et al. [43], where the arc lengths of the loops were kept fixed and which Avron et al. termed a necklace of rings.

5 Summary and future directions

After a brief discussion of a two-dimensional square lattice with a band potential which permits analytic solution, examples are given of the QN energy band dispersion relations in a graphene layer, and the corresponding density of states. A related B layer is also considered, followed by a discussion of the electronic structure of B nanotubes of different chiralities.

Some attention is then given to the effect of disorder of a QN model. Using a tree assumption (no closed circuits), a Boltzmann equation is derived for the logarithmic derivative of the density of states. Approximate analytic solutions are summarized, which subsequently can be refined numerically by the use of finite difference approximations, should this eventually prove necessary.

As to future directions, the work of Klein and March [7] points the way to important refinements, by returning to bond potentials. It may be that one can then reproduce the exact electron density along the wires (bonds) of the Kirchhoff network model, by use of the so-called Pauli potential introduced to allow a Schrödinger equation to be written for the bond density amplitude. Finally, for a disordered QN, the study of Ringwood [21] using random walk theory, which we have used numerically in Sect. 4 above, may point the way to a richer account of the effect of disorder on the nature of the electron states in a QN model.

Acknowledgements N.H.M. acknowledges that his contribution to this article was aided greatly by visits to the Abus Salam Centre International Centre for Theoretical Physics. He wishes to thank Professor V. E. Kravtsov for generous hospitality. The authors are also indebted to Professors P. Exner and P. Schrader for valuable discussions and helpful correspondence in bringing the article to fruition. In particular N.H.M. thanks Professor R. Schrader for drawing his attention to Ref. [20]. NHM was partially supported by the University of Antwerp through the BOF-NOI.

References

1. J.R. Platt, K. Ruedenberg, C.W. Scherr, N.S. Ham, H. Labhart, W. Lichten, *Free-Electron Theory of Conjugated Molecules: A Source Book* (Wiley, New York, 1964)
2. L. Pauling, J. Chem. Phys. **4**, 673 (1936)
3. C.A. Coulson, Proc. Phys. Soc. A **67**, 608 (1954)
4. C.A. Coulson, Proc. Phys. Soc. A **68**, 1129 (1955)
5. E.W. Montroll, J. Math. Phys. **11**, 635 (1970)
6. E.W. Montroll, J. Phys. Chem. Solids **34**, 597 (1973)
7. D.J. Klein, N.H. March, J. Mol. Struct. (Theochem) **337**, 257 (1995)
8. K.S. Novoselov, A.K. Geim, S.V. Morozov, D. Jiang, Y. Zhang, S.V. Dubonos, I.V. Grigorieva, A.A. Firsov, Science **306**, 666 (2004)
9. K.S. Novoselov, A.K. Geim, S.V. Morozov, D. Jiang, M.I. Katsnelson, I.V. Grigorieva, S.V. Dubonos, A.A. Firsov, Nature **438**, 197 (2005)
10. K.S. Novoselov, D. Jiang, F. Schedin, T.J. Booth, V.V. Khotkevich, S.V. Morozov, A.K. Geim, Proc. Natl. Acad. Sci. **102**, 10451 (2005)
11. M.I. Katsnelson, Mater. Today **10**, 20 (2007)
12. P. Kuchment, O. Post, Commun. Math. Phys. **275**, 805 (2007)
13. J. Dancz, S.F. Edwards, N.H. March, J. Phys. C **6**, 873 (1973)
14. F. Germinet, P.D. Hislop, A. Klein, J. Eur. Math. Soc. **9**, 577 (2007)
15. M. Aizenman, A. Elgart, S. Naboko, J.H. Schenker, G. Stolz, Invent. Math. **163**, 343 (2005)
16. M. Aizenman, R. Sims, S. Warzel, Probab. Theory Rel. Fields **136**, 363 (2006)
17. M. Aizenman, S. Warzel, Moscow Math. J. **5**, 499 (2005)
18. I. Veselić, Contemp. Math. **340**, 97 (2004), preprint `arXiv:math-ph/0307062`
19. P. Exner, M. Helm, P. Stollmann, Rev. Math. Phys. **19**, 923 (2006)
20. V. Kostrykin, R. Schrader, Waves Random Media **14**, S75 (2004)
21. G.A. Ringwood, J. Math. Phys. **22**, 96 (1981)
22. A.B. Budgor, J. Math. Phys. **17**, 1538 (1976)
23. F.E. Leys, C. Amovilli, N.H. March, J. Chem. Inf. Comput. Sci. **44**, 122 (2004)
24. R. Saito, G. Dresselhaus, M.S. Dresselhaus, *Physical Properties of Carbon Nanotubes* (Imperial College Press, London, 1998)

25. F.E. Leys, C. Amovilli, N.H. March, J. Math. Chem. **36**, 93 (2004)
26. A. Badanin, J. Brüning, E. Korotyaev, I. Lobanov (2007), preprint arXiv:0707.3909
27. A. Badanin, J. Brüning, E. Korotyaev (2007), preprint arXiv:0707.3900
28. I. Cabria, J.A. Alonso, M.J. López, Phys. Status Solidi (a) **203**, 1105 (2006)
29. S.H. Vosko, L. Wilk, M. Nusair, Can. J. Phys. **58**, 1200 (1980)
30. J.P. Perdew, J.A. Chevary, S.H. Vosko, K.A. Jackson, M.R. Pederson, D.J. Singh, C. Fiolhais, Phys. Rev. B **46**, 6671 (1992)
31. J.M. Ziman, J. Phys. C **6**, L361 (1973)
32. J. Dancz, S.F. Edwards, J. Phys. C **6**, 3413 (1973)
33. J. Dancz, S.F. Edwards, J. Phys. C **8**, 2532 (1975)
34. K. Ruedenberg, Ch. W. Scherr, J. Chem. Phys. **21**, 1565 (1953), [**22**, 151 (1954)]
35. Ch. W. Scherr, J. Chem. Phys. **21**, 1582 (1953)
36. J.R. Platt, J. Chem. Phys. **21**, 1597 (1953)
37. Ch. W. Scherr, J. Chem. Phys. **21**, 1413 (1953)
38. H.L. Frisch, S.P. Lloyd, Phys. Rev. **120**, 1175 (1960)
39. B.I. Halperin, Phys. Rev. **139**, A104 (1965)
40. P. Lloyd, J. Phys. C **2**, 1717 (1969)
41. F. Germinet, A. Klein, Commun. Math. Phys. **222**, 415 (2001)
42. P. Stollmann, *Caught by Disorder. Bound States in Disordered Media, Progress in Mathematicl Physics* (Birkhäuser, Boston, 2001)
43. J. Avron, P. Exner, Y. Last, Phys. Rev. Lett. **72**, 896 (1994)